



# Fuel Performance Modeling Plan to Support the Advanced Gas Reactor Program

March 2022

William F. Skerjanc



*INL is a U.S. Department of Energy National Laboratory  
operated by Battelle Energy Alliance, LLC*

#### **DISCLAIMER**

This information was prepared as an account of work sponsored by an agency of the U.S. Government. Neither the U.S. Government nor any agency thereof, nor any of their employees, makes any warranty, expressed or implied, or assumes any legal liability or responsibility for the accuracy, completeness, or usefulness, of any information, apparatus, product, or process disclosed, or represents that its use would not infringe privately owned rights. References herein to any specific commercial product, process, or service by trade name, trademark, manufacturer, or otherwise, does not necessarily constitute or imply its endorsement, recommendation, or favoring by the U.S. Government or any agency thereof. The views and opinions of authors expressed herein do not necessarily state or reflect those of the U.S. Government or any agency thereof.

# **Fuel Performance Modeling Plan to Support the Advanced Gas Reactor Program**

**William F. Skerjanc**

**March 2022**

**Idaho National Laboratory  
Advanced Reactor Technologies  
Idaho Falls, Idaho 83415**

**<http://www.art.inl.gov>**

**Prepared for the  
U.S. Department of Energy  
Office of Nuclear Energy  
Under DOE Idaho Operations Office  
Contract DE-AC07-05ID14517**

*Page intentionally left blank*

## INL ART Program

# Fuel Performance Modeling Plan to Support the Advanced Gas Reactor Program

INL/RPT-22-66390

March 2022

### Technical Reviewer:

*Wen Jiang*

Wen Jiang  
Computational Scientist

03/16/2022

Date

### Approved by:

*Paul Demkowicz*

Paul A. Demkowicz  
AGR Fuels Technical Director

3/15/2022

Date

*Gerhard Strydom*

Gerhard Strydom  
INL ART Director

3/16/22

Date

*Michelle Sharp*

Michelle T. Sharp  
INL Quality Assurance

3/16/22

Date

## **ABSTRACT**

This report documents the current status of the fuel performance modeling initiative to support the Advanced Gas Reactor (AGR) program in the development of tristructural-isotropic-coated fuel particles. It includes a brief summary of the codes that have been developed to support tristructural isotropic modeling along with a summary of the behavior of fuel particles during irradiation and the modeling used to capture these effects. In addition, this report identifies further modeling and material property needs for further development based on experience from previously performed AGR experiments.

In general, the remaining activities to support fuel performance modeling for the AGR program include continued AGR experiment support for AGR-3/4 and AGR-5/6/7 as well as modeling improvements identified throughout the course of the program. These modeling improvements can be summarized as fission product transport and thermomechanical particle behavior.

Additional modeling needs may be identified while processing the data collected during the AGR post-irradiation examination campaign and may lead to further improvements that are not included in this report.

*Page intentionally left blank*

## CONTENTS

ABSTRACT.....	iv
ACRONYMS.....	ix
1. INTRODUCTION.....	1
1.1 Background.....	1
1.2 AGR Program .....	1
2. FUEL PERFORMANCE MODELING CODES.....	2
2.1 PARFUME.....	2
2.2 Bison .....	4
3. TRISO-COATED FUEL PARTICLES .....	5
3.1 Fuel Particle Behavior.....	5
3.2 Fuel Failure Mechanisms .....	6
4. AGR EXPERIMENT SUPPORT .....	7
4.1 AGR-3/4 Experiment.....	7
4.1.1 Post-Irradiation Examination .....	7
4.2 AGR-5/6/7 Experiment.....	8
4.2.1 Safety Test Predictions.....	8
4.2.2 Model Predictions Versus PIE Data on In-Pile Performance Comparison.....	9
4.2.3 Safety Test .....	9
4.3 TRISO Particle Kernel and Buffer Volume Fraction Margin.....	9
5. FUEL PERFORMANCE MODELING IMPROVEMENTS.....	9
5.1 Fission Product Transport Model.....	9
5.2 Thermomechanical Buffer Layer Modeling.....	11
5.2.1 Background.....	11
5.2.2 Buffer-IPyC Debonding.....	11
5.2.3 IPyC Cracking and SiC Failure.....	12
5.2.4 SiC-OPyC and OPyC-Matrix Bonding.....	14
5.2.5 Discussion .....	14
5.3 Pyrocarbon Creep Rate .....	15
6. OTHER ACTIVITIES .....	16
7. SUMMARY .....	17
8. REFERENCES.....	17

## FIGURES

Figure 1. PARFUME calculation flow chart. ....	3
------------------------------------------------	---



Figure 2. Monte Carlo methodology for calculating failure probability in Bison. ....	4
Figure 3. Typical TRISO-coated fuel particle geometry. ....	5
Figure 4. Behavior of coating layers in fuel particles. ....	6
Figure 5. Bison 2D axisymmetric model of FP transport. ....	10
Figure 6. Temperature profiles for the above boundary conditions. ....	11
Figure 7. AGR-1 irradiated particle with an asymmetrical buffer-IPyC gap from Ploger et al. [32]. ....	12
Figure 8. X-ray tomogram of an AGR-1 particle that experienced SiC failure, showing partial detachment of the buffer and IPyC layers and IPyC cracking at a point where the buffer-IPyC interface transitions from attached to separated (lower right), along with region of degraded SiC, from Hunn et al. [24]. ....	13
Figure 9. X-ray tomogram of an AGR-1 particle that experienced SiC failure, showing a buffer fracture aligned with an IPyC fracture in a region where the buffer-IPyC interface is intact, from Hunn et al. [24]. ....	13
Figure 10. Pyrocarbon irradiation-induced creep correlation coefficients. ....	15

## TABLES

Table 1. AGR-3/4 temperature boundary conditions. ....	10
Table 2. Measured failure fractions and upper bounds at 95% confidence for the AGR-1 and AGR-2 irradiation tests [22, 23]. ....	14
Table 3. AGR-5/6/7 predicted fuel particle failure using PARFUME. ....	16
Table 4. Fuel performance modeling plan summary. ....	17

*Page intentionally left blank*

## ACRONYMS

AGR	Advanced Gas Reactor
ATR	Advance Test Reactor
DLBL	deconsolidation-leach-burn-leach
DOE	Department of Energy
DTF	designed-to-fail
FP	fission product
HTGR	high-temperature gas-cooled reactor
INL	Idaho National Laboratory
IPyC	inner pyrolytic carbon
LEU	low enriched fuel
NEUP	Nuclear Energy University Program
OPyC	outer pyrolytic carbon
PARFUME	PARticle FUEl ModEl
PIE	post-irradiation examination
SiC	silicon carbide
TRISO	tristructural isotropic

*Page intentionally left blank*

# 1. INTRODUCTION

Fuel performance modeling assists in the fuel design, fabrication, optimization, experiment design, and understanding of fuel behavior under normal and accident conditions. The quality of the fuel performance modeling relies not only on the validity of the code but also the material properties associated with the fuel type in question, both during reactor operation and safety analyses. The extreme environment the fuel is subjected to, along with the complex coupled multidimensional physiochemical and thermomechanical phenomena, make modeling advanced fuel forms difficult.

This report documents the current status of the fuel performance modeling initiative to support the Advanced Gas Reactor (AGR) program in the development of tristructural isotropic (TRISO) coated fuel particles. A brief summary of the modeling codes that have been developed to support TRISO modeling is included along with a summary of fuel particle behavior during irradiation and the modeling used to capture these effects. In addition, this report identifies further modeling and material property needs for further development based on experience from past AGR experiments.

## 1.1 Background

The performance of the TRISO-coated fuel particle and the manufacturing quality level are critical to the success of modular high-temperature gas-cooled reactors (HTGRs). The TRISO-coated particle fuel design has existed since the 1960s as the preferred fuel technology for use in HTGRs. These fuel particles are characterized by a superior fission-product containment capability up to temperatures reached in the worst accident scenarios.

Coated-particle fuel consists of spherical kernels—less than a millimeter in diameter—of oxide, carbide, or oxycarbide (a mixture of oxide and carbide) fuel encased in multiple coating layers: a porous carbon buffer, a dense inner layer of pyrolytic carbon (IPyC), a silicon carbide (SiC) layer, and an outer pyrolytic carbon layer (OPyC). The SiC layer is the most important part of the coating layer containment system. It is the primary load bearer of internal pressure from fission gas and carbon monoxide potentially created by the reaction of excess oxygen released from fission of uranium dioxide with the buffer, and it is the primary barrier to the release of fission products. The shrinkage of the dense PyC layers with increasing fast neutron fluence imparts a compressive stress on the SiC layer sandwiched between them, significantly reducing the peak tensile stress that can be attained in the SiC layer during irradiation. Both PyC layers also act as retention barriers to fission gases. Finally, the buffer provides a void volume to accommodate fission gases and carbon monoxide, which helps reduce the deleterious pressure buildup. The buffer also attenuates fission-product recoils, which protects the IPyC layer, and it accommodates kernel swelling during irradiation.

A multitude of phenomena have been historically observed in TRISO-coated fuel particles undergoing irradiation, leading to the identification of failure mechanisms (i.e., failure of one or more coating layers). Models have been subsequently developed to accurately simulate these failure mechanisms with the intent of mitigating them through adequate fuel design (e.g., by optimizing particle geometry) or careful choice of irradiation conditions.

## 1.2 AGR Program

The Department of Energy (DOE) AGR Fuel Development and Qualification Program was established to qualify TRISO-coated fuel for use in HTGRs. The primary goal of the program is to provide a baseline fuel qualification data set in support of the licensing and operation of an HTGR [1].

Seven fuel and material irradiation experiments are planned for the DOE AGR program. The overall objectives of these experiments are to [1]:

- Develop fuel fabrication capabilities
- Perform fuels and materials irradiation

- Perform safety testing and post-irradiation examination (PIE)
- Improve fuel performance modeling
- Evaluate fission product transport and source term determination.

Fuel performance modeling is critical to the success of the AGR program. This program element addresses the structural, thermal, and chemical processes that can lead to TRISO-coated particle failures and considers the effects of fission product chemical interactions with the coatings, which can lead to the degradation of the coated particle properties. Fission product release from the fuel particles and transport in the fuel-compact matrix and fuel-element graphite during irradiation are also modeled. Computer codes and models will be further developed and validated as necessary to support fuel fabrication process development [1].

Fuel performance modeling, as it relates to the AGR program, consists of the following [1]:

- Improve the existing coated-particle material property database to help develop constitutive relations that describe the thermomechanical, thermophysical, and physiochemical behavior of coated particles
- Develop a mechanistic fuel performance model for normal and off-normal HTGR conditions and benchmark against relevant performance data.

## **2. FUEL PERFORMANCE MODELING CODES**

To support this program element, Idaho National Laboratory (INL) has developed PARTicle FUEL Model (PARFUME) a fuel performance modeling code. Subsequently, INL developed the modeling code Bison using the Multiphysics Object-Oriented Simulation Environment finite element library. A brief description of the two codes follows.

### **2.1 PARFUME**

PARFUME is an integrated mechanistic computer code that evaluates the thermal, mechanical, and physicochemical behavior of coated fuel particles and the probability for fuel failure given the particle-to-particle statistical variations in physical dimensions and material properties that arise during the fuel fabrication process [2]. PARFUME describes both the mechanical and physicochemical behavior of the fuel particle under irradiation and postulated accident conditions, while capturing the statistical nature of the fuel and determines the failure probability of a population of fuel particles, accounting for all viable mechanisms that can lead to particle failure. In addition, PARFUME calculates fission product (FP) transport and accounts for these particle failures by determining the diffusion of fission products from the fuel through the particle coating layers and their subsequent release through the fuel matrix to the coolant boundary. The general solution procedure used by PARFUME consists of the basic processes depicted in the flow chart of Figure 1.

Coated particle fuel exhibits statistical variations in physical dimensions and material properties from particle to particle due to the nature of the fabrication process. Particle behavior is also inherently multidimensional, further complicating model development. The failure probability of a batch of fuel particles depends on statistical variations in the fuel design parameters as well as variation in the characteristic strengths of the coating layers in a batch. The calculation of fuel particle failures implemented in PARFUME samples the fuel design parameters from a Gaussian statistical distribution, and the layer strengths are sampled from a Weibull statistical distribution [3, 4]. PARFUME allows for statistical variations in the kernel diameter, the four-layer thicknesses, the pyrocarbon densities, the degree of anisotropy of the pyrocarbons (as measured by the Bacon anisotropy factor), the creep coefficient for the pyrocarbon, Poisson's ratio in creep for the pyrocarbon, bond strength between the IPyC and SiC layers, and particle asphericity (as measured by the aspect ratio).

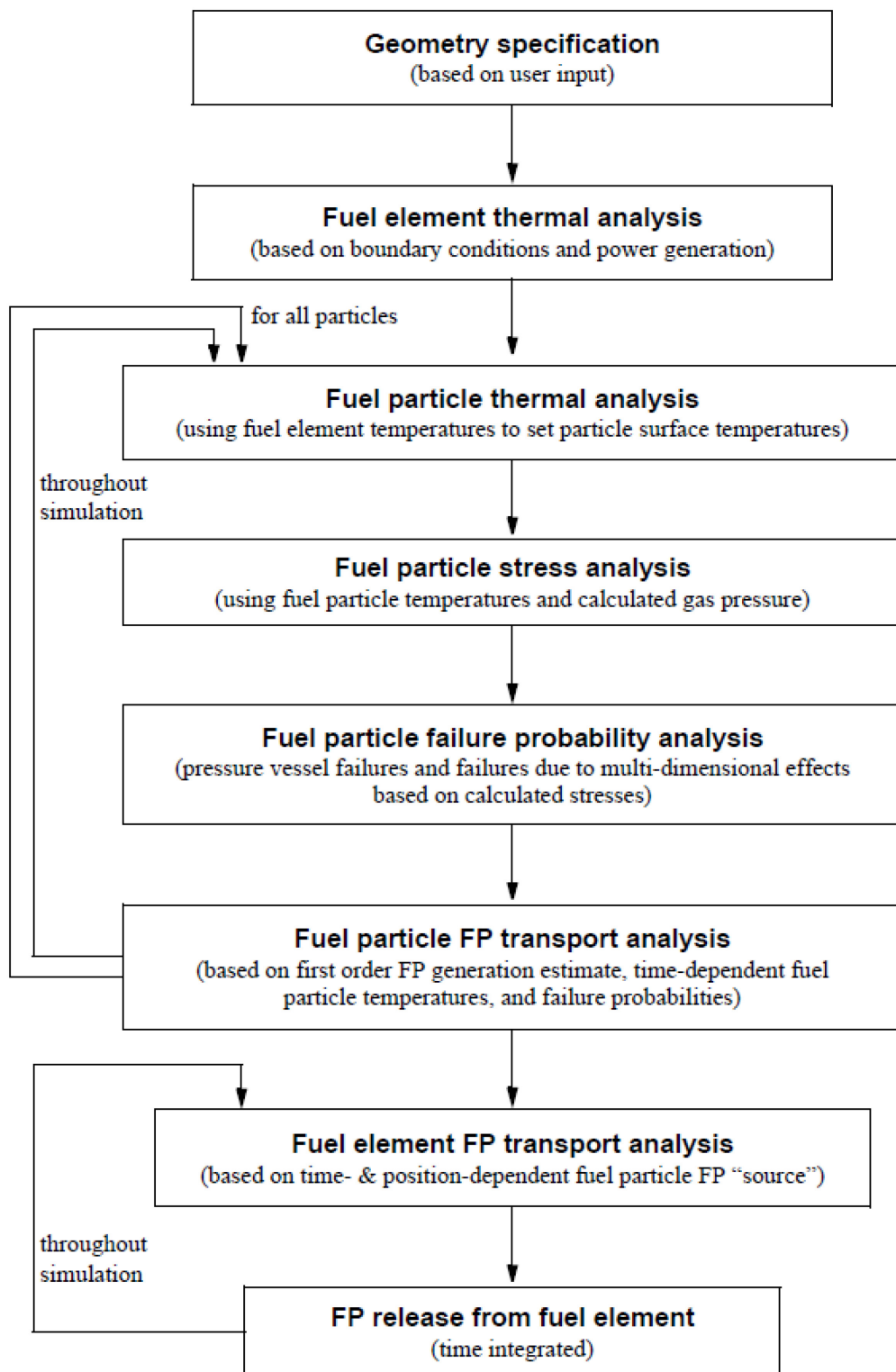


Figure 1. PARFUME calculation flow chart.

## 2.2 Bison

Bison [5] is a nuclear fuel performance application built using the Multiphysics Object-Oriented Simulation Environment finite element library [6] developed at INL that is capable of modeling multiple fuel forms in a wide variety of dimensions and geometries. It solves coupled nonlinear partial differential equations, including heat conduction, mechanics, FP species transport, etc., in a fully implicit manner. More detailed descriptions of the Bison fuel performance code as it relates to TRISO fuel modeling can be found in “Bison TRISO Modeling Advancements and Validation to AGR-1 Data” [7], “Numerical Evaluation of AGR-2 Fission Product Release” [29], and “TRISO particle fuel performance and failure analysis with Bison” [8]. The Monte Carlo methodology used in Bison to calculate the failure probability of a batch of fuel particles is summarized in Figure 2 [8]. Recently, a more efficient statistical failure analysis, similar to the “fast” integration methodology in PARFUME, has been added to Bison [30].

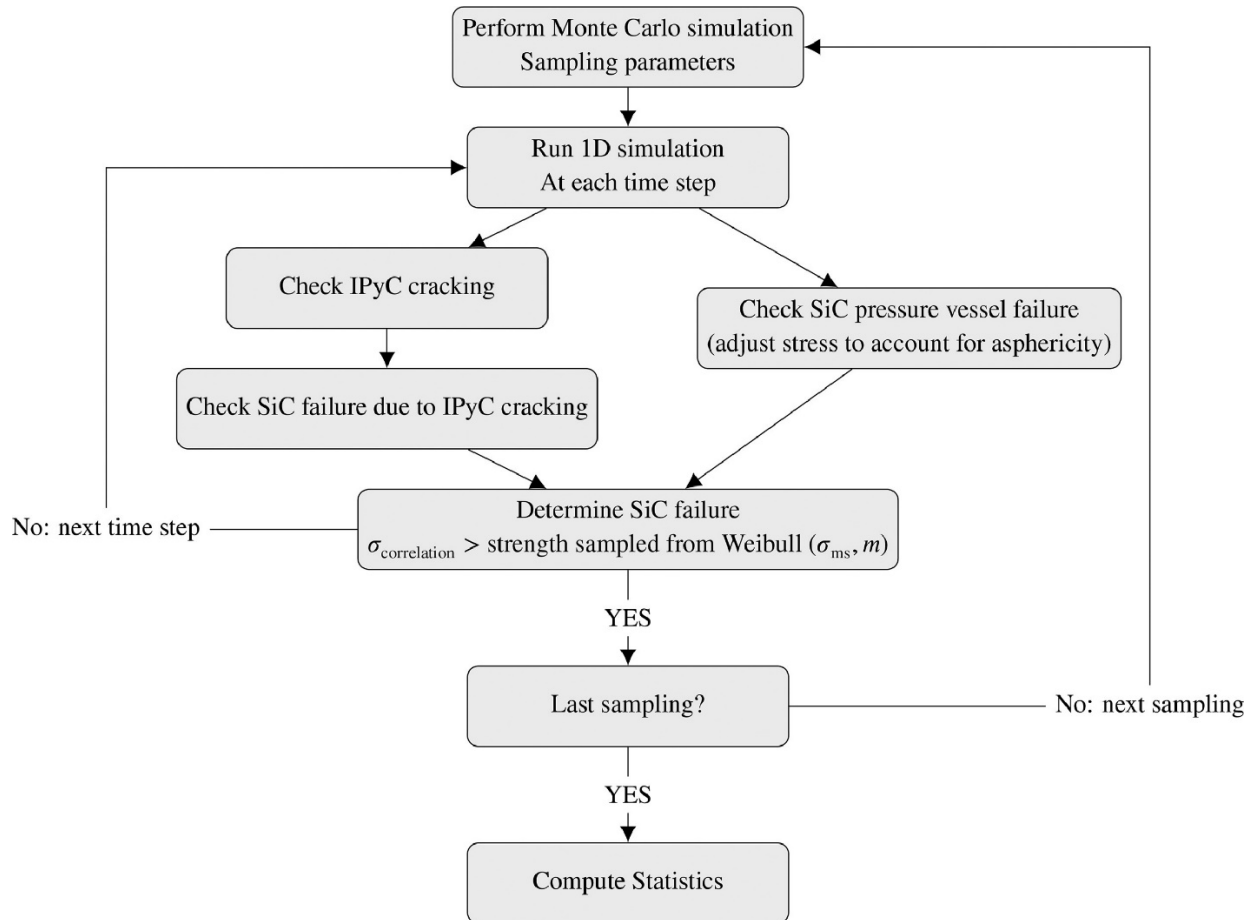


Figure 2. Monte Carlo methodology for calculating failure probability in Bison.

Bison can easily incorporate different irradiation conditions and run either very small analyses with a single processor or very large analyses on multiple processors on a supercomputer. For TRISO fuel, Bison supports spherically symmetric models, axisymmetric models, and fully 3D models. Thermomechanical models for each material layer includes elastic, irradiation creep, irradiation-induced dimension change, thermal expansion, and thermal conductivity.



FP generation, diffusion, and release can also be modeled for TRISO particles with uranium dioxide ( $\text{UO}_2$ ), uranium oxycarbide (UCO) and uranium nitride kernels. In addition, Bison has the ability to perform statistical failure analyses of large samples of fuel particles. This capability enables the evaluation of failure due to multidimensional failure phenomena by analyzing thousands of particles. This enables realistic calculations of the fission product release from the many particles in a TRISO-fueled reactor.

### 3. TRISO-COATED FUEL PARTICLES

The AGR program has selected the UCO fuel kernel (as opposed to  $\text{UO}_2$ ) due to its superior performance at high temperatures during irradiation and at high burnup ( $>12\%$  fissions per initial metal atom). A brief description of a typical TRISO-coated fuel particle follows, along with the potential failure mechanisms under consideration for modeling purposes. A more detailed description of potential failure mechanisms is provided in the “Technical Program Plan for INL Advanced Reactor Technologies Advanced Gas Reactor Fuel Development and Qualification Program” [1].

#### 3.1 Fuel Particle Behavior

A TRISO-coated particle is shown schematically in Figure 3. Several physical phenomena influence particle behavior, including fission gas production and irradiation effects. For example, fission gas pressure builds up in the kernel and buffer regions, while the IPyC, SiC, and OPyC act as structural layers to retain this pressure. The basic fuel behavior during irradiation is shown schematically in Figure 4, where the IPyC and OPyC layers both shrink and creep due to irradiation of the particle, while the SiC response is essentially limited to elastic behavior. The pressure generally increases as the irradiation of the particle progresses, thereby contributing to a tensile hoop stress in the SiC layer. The shrinkage of the IPyC during irradiation counters the effect of the pressure load by pulling inward on the SiC. Likewise, OPyC shrinkage causes it to push inward on the SiC. Particle failure is expected if the stress in the SiC layer reaches its fracture strength. SiC failure results in an instantaneous release of elastic energy that should be sufficient to cause the simultaneous failure of the pyrocarbon layers. These effects are described using material, thermal, and physicochemical models.

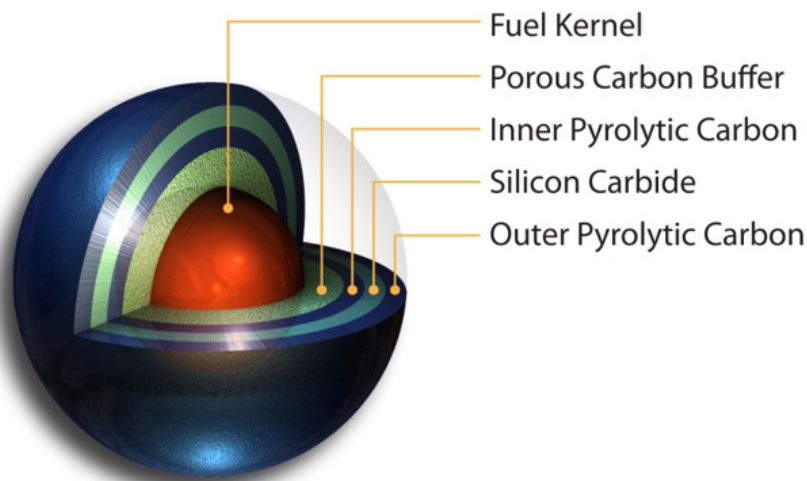


Figure 3. Typical TRISO-coated fuel particle geometry.

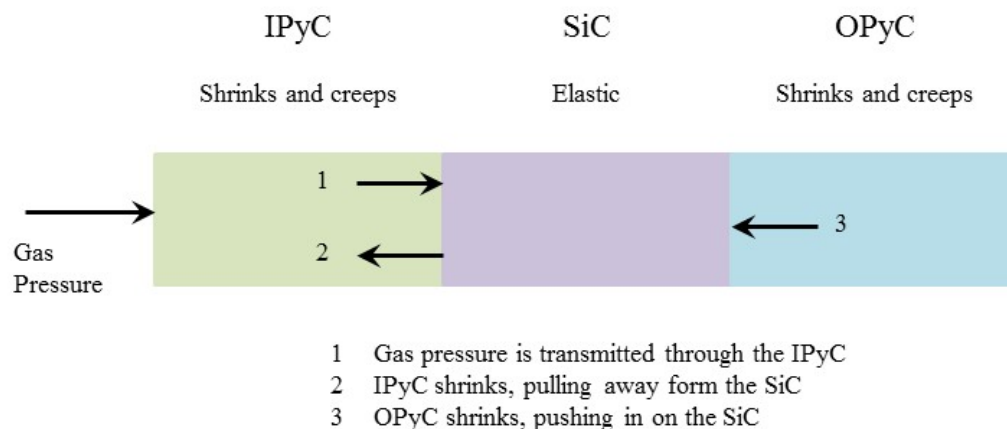


Figure 4. Behavior of coating layers in fuel particles.

## 3.2 Fuel Failure Mechanisms

Weibull statistical theory is used to determine whether particles fail using a mean strength for the SiC layer based on a stress distribution corresponding to the failure mechanism under consideration. The failure modes are implemented such that a particle fails only in the mode of failure that would occur first for that particle. The code retains the time at which the failures occur, allowing for the construction of a time evolution of the failure probability for a batch of fuel particles. Weibull parameters used to evaluate failures of the SiC layer and cracking of the IPyC layer are discussed in a CEGA Corporation report [9]. SiC layer failure is assumed to lead to full TRISO particle failure.

Five potential failure mechanisms are currently considered. The first is a pressure vessel failure caused by a buildup of gases (e.g., fission gas, carbon monoxide). Stresses for this failure mechanism are determined using the one-dimensional solution in PARFUME for a three-layer (IPyC-SiC-OPyC) particle. Fuel particle asphericity results in an increase in SiC stress that requires additional modeling using the finite element analysis code Abaqus [10] for this multidimensional behavior. Abaqus generates the multidimensional input required by PARFUME to correlate the stresses of an aspherical particle to a perfectly spherical particle using the PARFUME statistical methodology [11]. Since Bison is a finite element code, it is capable of modeling the 2D and 3D nature of this failure mechanism without the aid of an additional Abaqus calculation.

The second is SiC layer failure caused by the partial debonding of the IPyC from the SiC. Debonding, if it occurs, results from the IPyC shrinking inward away from the SiC during irradiation. PARFUME first determines whether debonding between the layers occurs by comparing the radial stress between layers with the bond strength between layers. If debonding has occurred, the code estimates the stress in the SiC layer and accounts for the multidimensional effects using a previously documented methodology [11]. The implementation of the IPyC-SiC debonding phenomenon is currently under development in Bison. Because AGR particle fabrication is based on German processes, the bond strength is representative for German particles (i.e., 100 MPa). At this bond strength, IPyC-SiC debonding is generally not predicted and therefore does not contribute to particle failures.

The third is the fuel kernel migration into the SiC layer under the influence of a temperature gradient (or the “amoeba” effect). This effect is driven by the production of carbon monoxide and is only possible with UO<sub>2</sub> kernels and is very limited with UCO kernels.

The fourth is a SiC layer failure caused by irradiation-induced shrinkage and the associated IPyC layer cracking. The presence of a crack creates a stress concentration in the SiC layer [12] that may or may not lead to total fuel particle failure. Since PARFUME is a one-dimensional fuel performance code

and the effects of an IPyC crack on a TRISO fuel particle are multidimensional, Abaqus [10] is used to generate the required PARFUME input to estimate the stresses in the particle using the PARFUME statistical methodology [13]. In evaluating failures caused by IPyC cracking, PARFUME first determines whether the IPyC layer cracks using the Weibull statistical theory. If the IPyC layer cracks, the particle is evaluated for SiC layer failure due to the presence of the crack. Similar to particle asphericity, Bison does not need the additional Abaqus analysis to perform the 2D modeling of this phenomenon [30].

The fifth is a chemical attack of the SiC layer by palladium (Pd), which is modeled in PARFUME and Bison by calculating the Pd penetration into the SiC layer. The penetration rate is calculated by an Arrhenius function fitted to all available in-reactor data for Pd penetration in SiC [2]. Failure occurs when penetration through the SiC layer is complete, leading to the direct release of FPs. In actuality, the fuel particle would more than likely to fail prior to reaching a 100% Pd penetration, and a limit can be applied to the fuel performance criteria to establish a bounding limit on Pd penetration. This failure phenomenon has also been developed in Bison.

## **4. AGR EXPERIMENT SUPPORT**

The AGR program—including irradiation experiments and collection of PIE data—has been an integral part of the TRISO-coated fuel qualification for use in high-temperature reactors. Further, the data collected during these experiments has been used for the verification and validation of the codes that analyze the performance and integrity of these fuels. Comparisons between previous AGR experiments and PARFUME have been completed to both improve its modeling capabilities and identify gaps between the actual performance and analytic models. This work will continue for last two AGR irradiation campaigns, AGR-3/4 and AGR-5/6/7, using both PARFUME and Bison, to create a high level of confidence in both fuel performance codes for further use in the qualification of TRISO fuel. The following is a summary of the planned work for the continued support of the AGR program.

### **4.1 AGR-3/4 Experiment**

AGR-3/4 combined the third and fourth in this series of planned experiments to test TRISO-coated, low-enriched uranium UCO fuel. As defined in the technical program plan for the INL Advanced Reactor Technologies AGR fuel program [1], the objectives of the AGR-3/4 experiment are to:

1. Irradiate fuel containing UCO designed-to-fail (DTF) fuel particles that will provide a known source of FPs for subsequent transport through compact matrix and structural graphite materials
2. Assess the effects of sweep gas impurities (such as CO, H<sub>2</sub>O, and H<sub>2</sub>) typically found in the HTGR primary coolant circuit on fuel performance and subsequent FP transport
3. Provide irradiated fuel and material samples for PIE and safety testing
4. Support the refinement of fuel performance and FP transport models with online, PIE, and safety test data.

Bison was used to model three compacts in the AGR-3/4 experiment using the manufactured TRISO-coated fuel particle and compact data using the as-run irradiation conditions [14]. This study identified that further modeling improvements were needed in Bison to accurately model both the failure probability and FP release across the gas gaps to collect the FPs. This will be accomplished using both PIE and heat-up test data on selected compacts using both PARFUME and Bison.

#### **4.1.1 Post-Irradiation Examination**

PARFUME has previously been used to model AGR-1 and AGR-2 PIE data to compare the predicted as-run modeling results with the experimental data [15, 16]. Due to the complexity of the experimental configuration of AGR-3/4, Bison will be used along with PARFUME to compare the data.

The compact FP inventory collected during PIE will be the result of both nondestructive and destructive sampling of selected compacts.

Nondestructive post-irradiation gamma scanning will be performed on all 48 fuel compacts to measure the retained silver (Ag-110m) from both the driver fuel and DTF particles. The retention fraction is the inventory measured in the compact divided by the total inventory of silver produced during irradiation, as calculated by as-run coupled neutronics and depletion models. The release fraction is then equal to 1 minus the retention fraction, and this data will be compared to the predicted release fraction by both PARFUME and Bison.

A deconsolidation-leach-burn-leach (DLBL) analysis method will be conducted on selected compacts to determine the amount of cesium (Cs-137) and strontium (Sr-90) retained within the compact outside of the SiC layers. The DLBL measurements include the contribution from the amount of FPs released through intact coatings but retained in the compact outside of the SiC layer, as well as FPs from uranium contamination in the OPyC and compact matrix. If any particles with failed SiC are present and not removed from the population before the burn-leach is performed, the inventory of the kernels from these particles will also be included in the post-burn-leach solutions and may greatly exceed the level of FPs attributed to diffusive release through intact coatings.

In addition, irradiated microsphere gamma analysis will be used to gamma count individual particles from these deconsolidated compacts to quantify their Ag-110m inventory. The normalized ratio of the measured to calculated silver inventory is determined for each particle by calculating the ratio of the measured Ag-110m inventory to the predicted inventory. The average retention fraction for each compact is then calculated by averaging the individual particle values. The average silver release fraction ( $1 - \text{“measured retention fraction”}$ ) per particle will then be compared to the values calculated by PARFUME and Bison.

Finally, the diffusion of FPs from the driver fuel and DTF particles through the compact matrix, and eventually collected in the capsule components outside of the compacts in each AGR-3/4 capsule, will be modeled using Bison due to the 2D analysis required for this geometry. The AGR-3/4 Irradiation Test Plan [17] identified temperature profiles across the compact, graphite rings, and sink. The modeling effort that is described in more detail in Section 5.1 will utilize the AGR-3/4 as-run temperature profiles.

## **4.2 AGR-5/6/7 Experiment**

As defined in the technical program plan for the AGR Fuel Development and Qualification Program [1], the objectives of the AGR-5/6/7 experiment are:

1. Irradiate reference design fuel containing low-enriched UCO TRISO fuel particles to support fuel qualification
2. Establish the operating margins for fuel beyond normal operating conditions
3. Provide irradiated fuel performance data and irradiate fuel samples for PIE and safety testing.

Similar to the previous AGR experiments, PARFUME will be used to model the AGR-5/6/7 irradiation experiment and subsequent data comparison with the PIE results. Bison will also be used in conjunction with PARFUME to continue the development and identify modeling needs. PARFUME has already been used to model the as-run irradiation of the AGR-5/6/7 experiment [25].

### **4.2.1 Safety Test Predictions**

PARFUME and Bison will be used to predict the fuel failure probability and diffusion of FPs during the planned safety tests as part of the AGR-5/6/7 PIE effort. Similar predictions have been performed previously for AGR-1 and AGR-2 [19, 20]. Results from the AGR-5/6/7 study will include fuel failure probability, Pd penetration, and fractional release of FPs.

#### **4.2.2 Model Predictions Versus PIE Data on In-Pile Performance Comparison**

The modeling performed to support the AGR-5/6/7 PIE effort will be similar to those described above for AGR-3/4 and previously completed for AGR-1 and AGR-2. This will include modeling the FP diffusion to experimental data obtained from nondestructive (gamma scanning) and destructive (DLBL) FP inventories. This will include silver (Ag-110), cesium (Cs-137), and strontium (Sr-90).

It is anticipated that the FP release modeling from AGR-3/4 will result in updated diffusion modeling parameters that will be implanted in PARFUME and/or Bison. The AGR-5/6/7 PIE data will be used test the application of these parameters for future modeling applications.

#### **4.2.3 Safety Test**

Post-irradiation safety tests will be performed on selected compacts at various temperature ranges to determine FP release at temperatures that bound accidents conditions. PARFUME and Bison will be used to calculate the FP release of silver (Ag-110), cesium (Cs-137), and strontium (Sr-90) using the heat-up conditions for these safety tests. These calculations were performed for both AGR-1 [21] and AGR-2 [16]. If available, the updated FP diffusion parameters derived from the AGR-3/4 experiment will be used in this analysis.

### **4.3 TRISO Particle Kernel and Buffer Volume Fraction Margin**

Previous studies have identified the manufacturing critical limit for the design of the AGR TRISO particle buffer layer thickness such that it can adequately absorb FP gases and carbon monoxide [31]. It was determined that the minimum buffer layer thickness in the AGR TRISO particle before experiencing an increase if fuel particle failure is approximately 50  $\mu\text{m}$ . The current AGR TRISO particle has a buffer layer thickness of approximately 100  $\mu\text{m}$ , leaving a sufficient design margin before fuel particle failure is expected to occur. This study will evaluate different kernel diameters with varying buffer layer thicknesses while maintaining the same compact packing fraction. This will allow for the potential for an increase in fissile fuel material per compact while maintaining sufficient margin before fuel particle failures are expected to occur due to having a thinner buffer layer.

## **5. FUEL PERFORMANCE MODELING IMPROVEMENTS**

Throughout the evolution of the AGR irradiation experiments, phenomena and material properties have been identified that need to be included in fuel performance codes to predict the behavior of TRISO-coated fuel particles more accurately during irradiation and under accident conditions. In an attempt to capture these effects and properties, the fuel performance codes PARFUME and Bison will require improvements in their respective modeling capabilities. The following sections have identified potential areas of improvement to more accurately complete fuel performance simulations to aid in fuel failure probability and FP diffusion predictions.

### **5.1 Fission Product Transport Model**

Each AGR-3/4 compact contains driver fuel particles and 20 DTF particles placed along its axial centerline. The fuel compacts are surrounded by three concentric annular rings of test material consisting of fuel-compact matrix material and fuel-element graphite. Figure 5 shows a Bison 2D axisymmetric model, with the 20 DTF particles placed in the center line and 1,793 randomly distributed driver particles hosted in the fuel compact. The four regions of the Bison model are fuel compact, matrix, graphite, and the sink. They are separated blocks without sharing nodes between their interfaces. The physical properties of the TRISO fuel particle including kernels and coating layers are randomly generated from a Monte Carlo simulation. At every time step, the FP and heat released from each particle is transferred to the compact as a point source. Those point sources are used in the compact model to drive the FP and thermal diffusion. In this 2D axisymmetric model, the point sources are treated as circular sources.

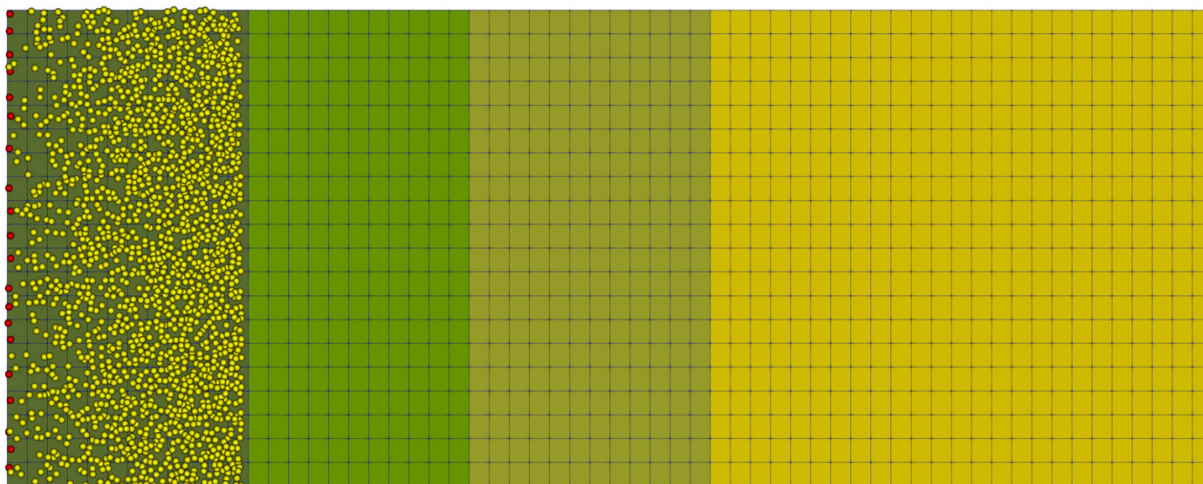


Figure 5. Bison 2D axisymmetric model of FP transport.

Temperature profiles determined using Abaqus and the interfacial conditions of FP diffusion are derived in “AGR-3/4 Irradiation Test Plan” [17] based on the sorption isotherm theory. The inner and outer temperature boundary conditions are set for each block using the values listed in Table 1 [17]. The resulting temperature profiles are shown in Figure 6 [17]. The AGR-3/4 irradiation experiment has been completed in the Advanced Test Reactor (ATR), and modeling FP diffusion will utilize the as-run temperature profiles. In addition to discontinuities in temperature, the presence of gas gaps also results in discontinuities of fission product concentration. The discontinuous interfacial conditions present a problem for traditional 1D fuel performance modeling codes, including PARFUME; therefore, Bison is currently being developed to accurately model the fission product diffusion across these gas gap discontinuities to predict the amount of fission products collected in the outer graphite sink.

Table 1. AGR-3/4 temperature boundary conditions.

Nominal Temp. (°C)	Compact Temp. (°C)	Matrix Temp. (°C)		Graphite Temp. (°C)		Sink Temp. (°C)	
	Outer	Inner	Outer	Inner	Outer	Inner	Outer
900	893	824	794	755	733	499	481
1100	1009	928	889	842	813	548	526
1250	1088	910	827	713	657	564	512
1400	1286	1125	1033	935	867	548	497

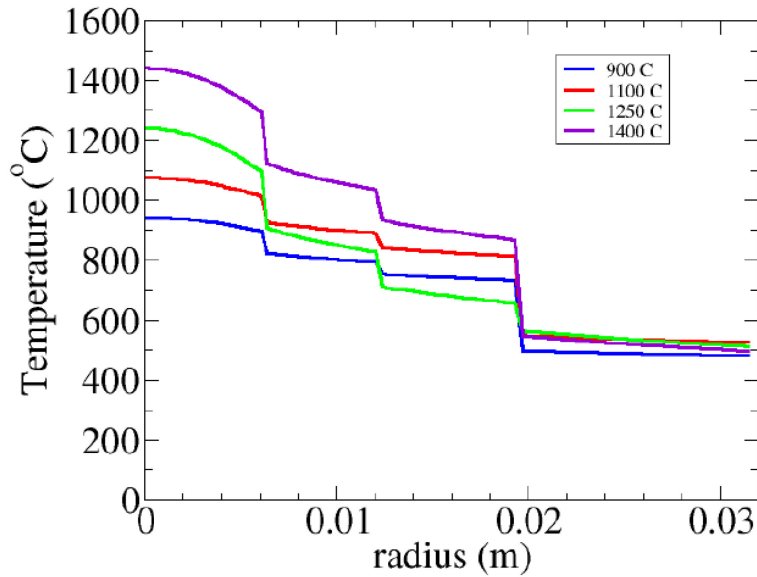


Figure 6. Temperature profiles for the above boundary conditions.

The new diffusion parameters derived from the AGR-3/4 PIE data will need to be validated versus experimental data. Numerous benchmarks have been performed that include AGR-1 and AGR-2 data sets for comparison. In addition, the new diffusion parameters can be used to model against measured PIE data obtained from the AGR-5/6/7. Combined, sufficient confidence will be obtained in the new diffusion parameters used for further TRISO-coated fuel performance predictions by both PARFUME and Bison.

## 5.2 Thermomechanical Buffer Layer Modeling

### 5.2.1 Background

The ongoing AGR PIE has included the examination of thousands of particles in cross section to observe irradiated kernel and coating morphologies (see the AGR-1 [22] and AGR-2 [23] final PIE reports for summaries of these results). The work as also involved extensive effort to locate particles with lower-than-normal fission product retention and examine these particles to identify any coating anomalies [24]. The particle characterization methods developed allow localized degraded regions of particles to be pinpointed and examined in detail and have greatly advanced the understanding of coating behavior during irradiation and causes of layer failure. Some of these empirical observations of particle behavior differ from the predicted or assumed behavior in the fuel performance models.

### 5.2.2 Buffer-IPyC Debonding

The buffer layer in the existing models is presumed to exhibit no adhesion to the IPyC layer, such that it can immediately detach as it begins to experience shrinkage during irradiation and create a growing gap between the buffer and IPyC layers. As a consequence of this behavior, the buffer layer does not exert any mechanical influence on the IPyC layer during irradiation in the models. PIE data indicate that the separation of the buffer and IPyC layers does not always happen immediately, and in many particles, a significant portion of the buffer-IPyC interface remains intact after hundreds of days of irradiation to burnup as high as  $\sim 19\%$  fissions per initial metal atom and a fast neutron fluence of  $\sim 5 \times 10^{25} \text{ n/m}^2$  ( $E \geq 0.18 \text{ MeV}$ ). This results in an asymmetric buffer-IPyC gap (Figure 7), the impact of which has not been examined in the models. A more important consequence of this behavior is that the buffer-IPyC interaction appears to affect the IPyC and SiC coating layer behavior, which is discussed below.



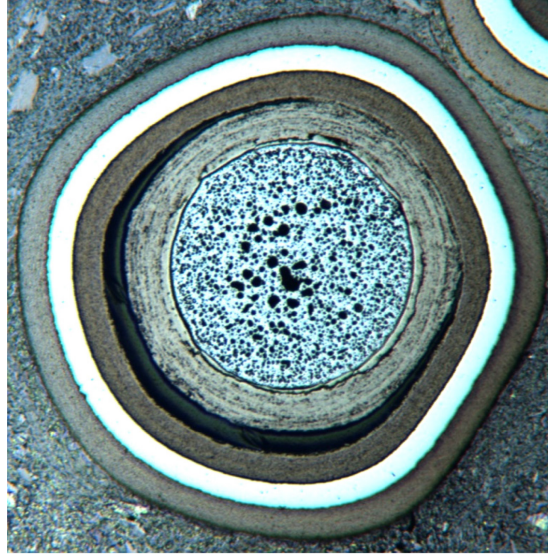


Figure 7. AGR-1 irradiated particle with an asymmetrical buffer-IPyC gap from Ploger et al. [32].

### 5.2.3 IPyC Cracking and SiC Failure

The extremely rare particles that experienced SiC layer failure during irradiation or during safety testing in the AGR-1 and AGR-2 experiments generally exhibited a similar failure mechanism, as described by Hunn et al. [24] and summarized here. Mechanical failure of the IPyC layer can expose a small region of the inner surface of the SiC layer to a localized fission product (primarily Pd) attack (Figure 8). Subsequently, sufficient time and temperature can result in complete through-layer degradation, such that Cs retention is compromised. A key observation is that particles exhibiting IPyC failure are often those where there is a significant portion of the buffer-IPyC interface that remains intact, and the IPyC layer failure occurs at a location where the buffer-IPyC interface transitions from intact to separated, as in Figure 8. These observations strongly suggest that dramatic buffer shrinkage (measured to be between 26–40 volume percent in irradiated AGR-1 and AGR-2 particles [24]) and that a relatively strong buffer-IPyC bond can increase the stress on the IPyC layer such that it promotes IPyC fracture and localized separation from the SiC layer. A second mode of IPyC fracture that has been observed is demonstrated in Figure 9, where a fracture in the buffer layer corresponds to a fracture in the IPyC layer in a region where the buffer-IPyC interface remains intact. In both cases, while the primary mode of SiC layer failure is fission product attack, the precursor to this is IPyC failure that may be significantly influenced by an interaction with the buffer layer.



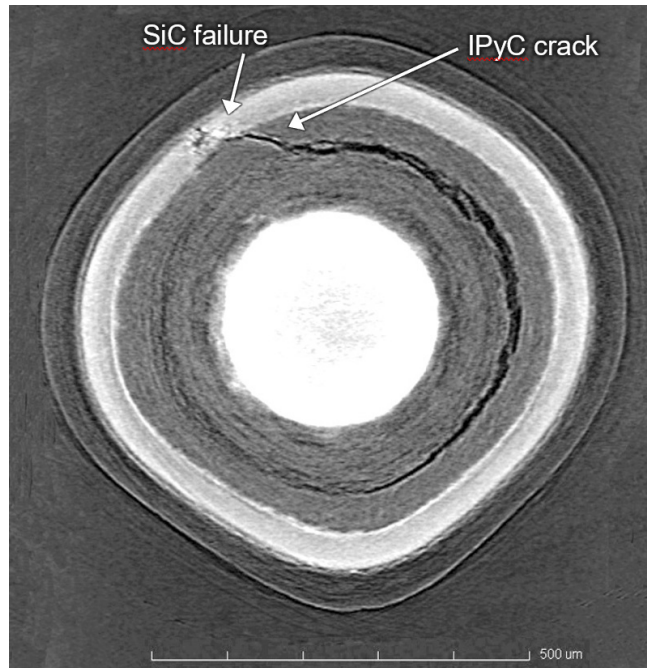


Figure 8. X-ray tomogram of an AGR-1 particle that experienced SiC failure, showing partial detachment of the buffer and IPyC layers and IPyC cracking at a point where the buffer-IPyC interface transitions from attached to separated (lower right), along with region of degraded SiC, from Hunn et al. [24].

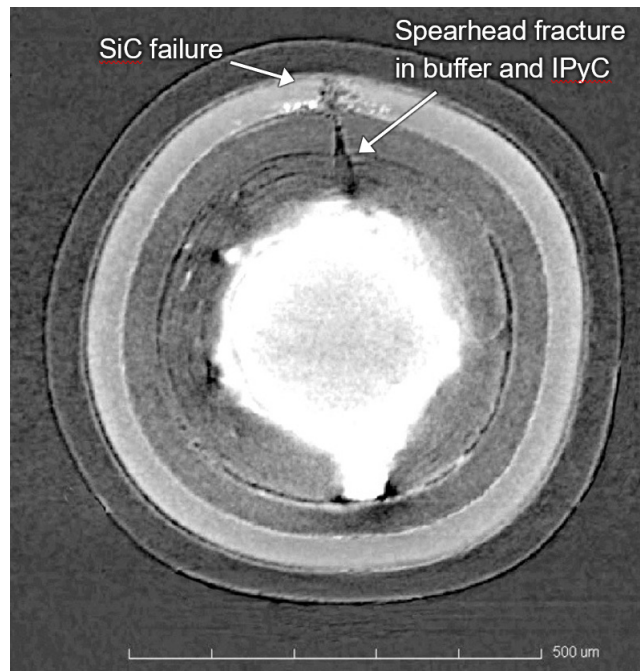


Figure 9. X-ray tomogram of an AGR-1 particle that experienced SiC failure, showing a buffer fracture aligned with an IPyC fracture in a region where the buffer-IPyC interface is intact, from Hunn et al. [24].

Accurate modeling of this behavior will be challenging due to the complexity of the behavior and a lack of necessary material properties. Among these properties are the strength of the buffer-IPyC bond and the mechanical properties of the buffer layer itself. Complicating the analysis is the observation that the buffer and IPyC layers do not always cleanly separate at the observable interface, but that portions of the buffer layer are often left on the IPyC layer following separation (i.e., the fracture takes place in the buffer near the layer interface).

#### 5.2.4 SiC-OPyC and OPyC-Matrix Bonding

Existing fuel performance models assume that the OPyC separates from the matrix layer, such that, when it experiences shrinkage due to irradiation, it remains bonded to the SiC layer and contributes to the compressive stress in it. However, some experimental observations of irradiated particles (with and without additional post-irradiation safety testing) indicate a small gap between the SiC and OPyC layers. This suggests that the OPyC layer may in fact remain bonded to the matrix while at the same time having a relatively weak bond with the SiC layer, allowing the OPyC to separate from the SiC layer due to OPyC or matrix shrinkage during high-temperature irradiation. This is somewhat consistent with observations of the as-deposited SiC surface and SiC-OPyC interface, which indicate that the outer SiC surface is relatively smooth with little topography that would allow the OPyC layer to interlock and form a strong bond, as occurs at the IPyC-SiC interface. This could have several implications for fuel performance models.

Firstly, it suggests that the OPyC may not contribute significantly to SiC compressive stress or that the contribution to the SiC stress is unpredictable. Secondly, it suggests that, upon the mechanical failure of the IPyC and SiC layers (such that the OPyC remains the only intact layer to retain the pressure generated from fission gas build up), it may not be appropriate to consider the stresses in the OPyC layer independent from the matrix. The existing model results in the immediate failure of the OPyC layer in these cases, since it does not have sufficient tensile strength to retain all of the stress previously retained by SiC layer. However, if the OPyC layer is not coupled to the SiC layer and is instead attached to the matrix, the approach to evaluate layer failure would be considerably different.

#### 5.2.5 Discussion

The experimentally observed failure rates of the AGR-1 and AGR-2 fuel particles are very low. Table 2 provides the measured failure fraction and upper bound on the failure fraction at 95% confidence for both SiC and TRISO failures for the AGR-1 and AGR-2 irradiations (additional details can be found in the respective final PIE reports [22, 23]). Note that “SiC failure” refers to a failure of the SiC layer such that it loses the ability to retain fission products (notably cesium) but with at least one PyC layer remaining intact to retain fission gases, while “TRISO failure” refers to the functional failure of all three dense coating layers such that fission gases are released from the particle.

Table 2. Measured failure fractions and upper bounds at 95% confidence for the AGR-1 and AGR-2 irradiation tests [22, 23].

Experiment	SiC Failures		TRISO Failures	
	Measured	Upper Bound at 95% Confidence	Measured	Upper Bound at 95% Confidence
AGR-1	$1.3 \times 10^{-5}$	$\leq 3.1 \times 10^{-5}$	0	$\leq 1.1 \times 10^{-5}$
AGR-2	$5.3 \times 10^{-5}$	$\leq 1.1 \times 10^{-4}$	$\leq 3.5 \times 10^{-5}$	$\leq 8.1 \times 10^{-5}$

Given the relatively low frequency of these coating layer failures and the large volume of fuel tested in the AGR program to demonstrate fuel performance (over 400,000 particles in the two tests represented in Table 1, with an additional ~500,000 particles from the AGR-5/6/7 experiment currently under PIE), an ample performance margin has been empirically demonstrated. As a result, capturing all of the nuanced impacts of coating performance in the models does not appear to represent a pressing concern with

respect to AGR-spec UCO low-enriched uranium TRISO particles under the AGR program irradiation conditions. However, the impact of these particle behaviors for fuel designs that deviate significantly from that tested in the AGR program, and under a significantly different performance envelope for which there are little or no empirical data, remains to be determined. In these cases, model refinement may prove to be more crucial.

An initial goal of future code development efforts will be to determine the feasibility of refining the models to incorporate observed behaviors. This will likely be dependent on the availability of updated materials properties (see additional discussion in Section 6) or adequate experimental data for the failure modes to be incorporated based on empirical correlations (e.g., rate of localized Pd attack of SiC in the event of IPyC failure).

### 5.3 Pyrocarbon Creep Rate

The irradiation-induced pyrocarbon creep consists of transient creep and steady-state creep. Due to the lack of established data and its minimal effect on particle stresses, transient creep is not included in PARFUME or Bison and only the steady-state creep is considered. The correlations used in the two fuel performance codes are only valid between 600 and 1350°C. If the irradiation temperature is below 600°C, the creep correlation is set to the value at 600°C. Similarly, if the temperature is above 1350°C, the coefficient is set to the value at 1350°C. The creep correlation used in PARFUME and Bison is illustrated in Figure 10 for various pyrocarbon densities ( $\rho$ ).

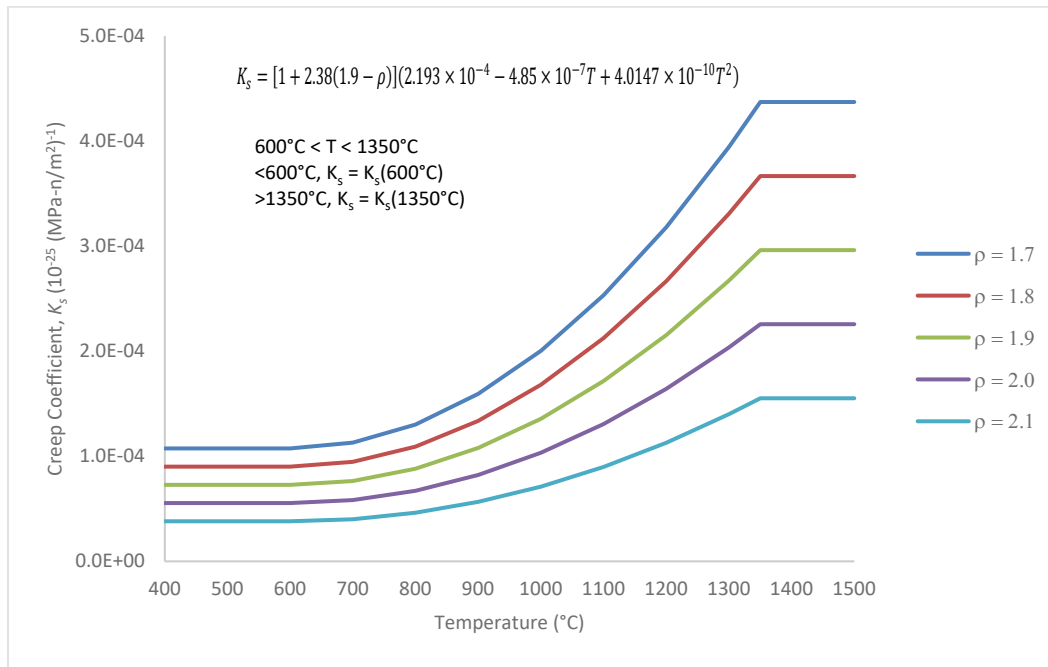


Figure 10. Pyrocarbon irradiation-induced creep correlation coefficients.

The irradiation-induced creep correlation is based on experimental data and derived in the CECA Corporation report, first published in 1993 [9]. Since then, the AGR program has performed graphite irradiation experiments and TRISO particle irradiations at lower temperatures that have shown that perhaps the creep correlation coefficients used in the two fuel performance codes may not be accurate at low temperatures. Although the creep coefficients used in the codes are conservative, an updated creep correlation would improve the accuracy of predicting fuel particle failures associated with IPyC cracking. This was demonstrated when predicting the fuel particle failures during AGR-5/6/7 irradiation using

PARFUME [25]. As summarized in Table 3, PARFUME overpredicted the number of fuel particle failures based on the average capsule failure fraction at lower temperatures. These fuel particle failures are due to localized stress concentrations caused by cracks in the IPyC layer caused by shrinkage in the layer and the creep not relieving the stresses early during the irradiation. More accurate irradiation-induced creep coefficients at lower temperatures will more accurately reflect the physical behavior of TRISO particles during irradiation.

Table 3. AGR-5/6/7 predicted fuel particle failure using PARFUME.

Capsule	5	4
Average compact temperature (°C)	741	839
Average compact predicted failure fraction	2.60E-04	1.14E-04
Total number of TRISO particles	81432	52728
Predicted number of TRISO particle failures	21	6
Observed number of TRISO particle failures <sup>1</sup>	0	0

1. Per AGR-5/6/7 irradiation as-run report [18] based on the data currently available.

## 6. OTHER ACTIVITIES

There are several activities being performed outside of the AGR program that support the overall objective of developing fuel performance modeling tools for TRISO-coated fuel particles. A number of high-temperature reactor vendors have been evaluating the use of TRISO-coated particles that rely on fuel performance modeling to support eventual fuel qualification. These reactor and fuel vendors depend on INL for the expertise and model developments of the AGR program. However, since the scope of their work and variations in both reactor and fuel design fall beyond the AGR program, they will not be discussed further in this report.

The Bison fuel performance code falls outside of the AGR program scope, but it has been under constant development for fuel performance modeling. This report attempts to capture the major activities directly related to the immediate support of the AGR program and is not all encompassing. Further, Bison is export-controlled software and many of the fuel vendors have developed some version of the Bison code to meet their needs. Since many of these modifications are business sensitive, they too are not included in this report.

The DOE's Nuclear Energy University Program (NEUP) supports university research and collaboration. Currently, there are two NEUP-funded projects that coincide with an application to fuel performance modeling. In an attempt to measure the material properties of TRISO layers and their interfaces, NEUP-19-17251 [26] has been awarded to Idaho State University to develop strength characterization techniques via tensile testing for unirradiated and irradiated TRISO-coated fuel for deployment to other collaborators. If the characterization of the TRISO layers is successful, PARFUME and Bison can be updated with new material properties for further investigation and comparison to the experimental data obtained throughout the AGR program.

Additionally, NEUP-20-19556 [27] has been awarded to the University of Wisconsin to develop a predictive model for the buffer layer performance during irradiation. In conjunction with data obtained from the AGR experiments and subsequent PIE, this research will help improve modeling capabilities in Bison when evaluating the buffer layer performance during irradiation. Since PARFUME is a 1D fuel performance code, the application of the buffer layer behavior is not anticipated to be included in its modeling capabilities.

Finally, the DOE's Integrated Research Projects program has awarded the University of Tennessee to develop computationally efficient multiphysics models in Bison for TRISO-coated fuel in advanced reactors [28]. The results of this research can be utilized in future versions of Bison for TRISO fuel performance modeling.

## 7. SUMMARY

In general, the remaining activities to support fuel performance modeling for the AGR program include the continued AGR experiment support for AGR-3/4 and AGR-5/6/7 as well as modeling improvements identified throughout the course of the program. These modeling improvements can be summarized as fission product transport and thermomechanical particle behavior.

Fission product transport modeling will be improved using the empirical data obtained from the AGR-3/4 PIE campaign. This will include implementation of new fission product diffusion parameters in both PARFUME and Bison. The implementation of these new diffusion parameters will need to be compared against AGR-1 and AGR-2 data as well as published fuel performance benchmarks.

Fuel particle thermomechanical behavior includes the improved modeling of the buffer layer during irradiation and potentially updating pyrocarbon creep coefficients at lower temperatures to reflect fuel particle failure observations more accurately during AGR-5/6/7. In addition, the AGR program has accumulated substantial experimental data on the behavior of fuel particles both during irradiation and under accident conditions. Processing this data may lead to the identification of further modeling improvements. For example, the physicochemical behavior of SiC layer corrosion by fission products has been observed and will need to be quantified to be included in fuel performance models.

Fuel performance modeling activities and improvements that have been identified in this report are summarized in Table 4, along with notional completion dates where applicable.

Table 4. Fuel performance modeling plan summary.

Activity	Modeling Code	Completion	Deliverable
AGR Experiment Support			
AGR-3/4 PIE and Safety Test Comparison	PARFUME/Bison	FY-22	INL Report
AGR-5/6/7 Safety Test Predictions	PARFUME/Bison	FY-23	INL Report
AGR-5/6/7 In-pile PIE Comparison	PARFUME/Bison	FY-24	INL Report
AGR-5/6/7 Safety Test Comparisons	PARFUME/Bison	FY-26	INL Report
AGR Kernel/Buffer Fraction Margin	PARFUME	FY-23	INL Report
<b>Modeling Improvements</b>			
Fission Product Transport Model	Bison	FY-23	INL Report
Thermomechanical Buffer Layer Modeling	Bison	TBD	INL Report
Pyrocarbon Creep Rate	PARFUME/Bison	TBD	INL Report
<b>Other Activities</b>			
NEUP-19-17251	PARFUME/Bison	TBD	
NEUP-20-19556	Bison	TBD	
IRP-20-22094	Bison	TBD	

## 8. REFERENCES

1. “Technical Program Plan for INL Advanced Reactor Technologies Advanced Gas Reactor Fuel Development and Qualification Program,” PLN-3636, Rev. 10, Idaho National Laboratory, June 22, 2021.
2. Miller, G. K., D. A. Petti, J. T. Maki, D. L. Knudson, W. F. Skerjanc. 2018. “PARFUME Theory and Model Basis Report,” INL/EXT-08-14497, Rev. 1, Idaho National Laboratory.  
<https://doi.org/10.2172/1471713>.

3. Kovacs, W. J., K. Bongartz, and D. T. Goodin. 1985. "High-Temperature Gas-Cooled Reactor Fuel Pressure Vessel Performance Models." *Nuclear Technology* 68: 344–354. <https://doi.org/10.13182/NT85-A33580>.
4. Martin, D. G. 2002. "Considerations Pertaining to the Achievement of High Burn-ups in HTR Fuel." *Nuclear Engineering and Design* 213: 241–258. [https://doi.org/10.1016/S0029-5493\(01\)00502-7](https://doi.org/10.1016/S0029-5493(01)00502-7).
5. Williamson, R. L., J. D. Hales, S. R. Novascone, G. Pastore, K. A. Gamble, B. W. Spencer, W. Jiang, S. A. Pitts, A. Casagrande, D. Schwen, A. X. Zabriskie, A. Toptan, R. Gardner, C. Matthews, W. Liu, and H. Chen. 2021. "Bison: A Flexible Code for Advanced Simulation of the Performance of Multiple Nuclear Fuel Forms." *Nuclear Technology* 207(7): 954–980. <https://doi.org/10.1080/00295450.2020.1836940>.
6. Permann, C. J., D. R. Gaston, D. Andrš, R. W. Carlsen, F. Kong, A. D. Lindsay, J. M. Miller, J. W. Peterson, A. E. Slaughter, R. H. Stogner, and R. C. Martineau. 2020. "MOOSE: Enabling Massively Parallel Multiphysics Simulation." *SoftwareX* 11: 100430. <https://doi.org/10.1016/j.softx.2020.100430>.
7. Hales, J. D. 2021. "Bison TRISO Modeling Advancements and Validation to AGR-1 Data." INL/EXT-20-59368, Rev. 0, Idaho National Laboratory. <https://doi.org/10.2172/1711423>.
8. Jiang, W., J. D. Hales, B. W. Spencer, B. P. Collin, A. E. Slaughter, S. R. Novascone, A. Toptan, K. A. Gamble, R. Gardner. 2021. "TRISO Particle Fuel Performance and Failure Analysis with Bison," *Journal of Nuclear Materials* 548: 152795. <https://doi.org/10.1016/j.jnucmat.2021.152795>.
9. "NP-MHTGR Material Models of Pyrocarbon and Pyrolytic Silicon Carbide," CECA-002820, Rev. 1, CECA Corporation, July 1993.
10. Abaqus, Abaqus User's Manual, Dassault Systemes Simulia Corp., 2009.
11. Miller, G. K., D. A. Petti, and J. T. Maki. 2004. "Consideration of the Effects of Partial Debonding of the IPyC and Particle Asphericity on TRISO-coated Fuel Behavior." *Journal of Nuclear Materials* 334(2–3): 79–89. <https://doi.org/10.1016/j.jnucmat.2004.04.330>.
12. Miller, G. K., D. A. Petti, D. J. Varacalle, and J. T. Maki. 2001. "Consideration of the Effects on Fuel Particle behavior from Shrinkage Cracks in the Inner Pyrocarbon Layer." *Journal of Nuclear Materials* 295(2–3): 205–212. [https://doi.org/10.1016/S0022-3115\(01\)00551-7](https://doi.org/10.1016/S0022-3115(01)00551-7).
13. Miller, G. K., D. A. Petti, D. J. Varacalle, and J. T. Maki. 2003. "Statistical Approach and Benchmarking for Modeling of Multi-dimensional behavior in TRISO-coated Fuel Particles." *Journal of Nuclear Materials* 317: 69–82. [https://doi.org/10.1016/S0022-3115\(02\)01702-6](https://doi.org/10.1016/S0022-3115(02)01702-6).
14. Skerjanc, W. F., J. Wen. 2021. "Bison As-run AGR-3/4 Irradiation Test Predictions," INL/EXT-21-65160, Rev. 0, Idaho National Laboratory.
15. Collin, B. P. 2014. "Comparison of Fission Product Release Predictions using PARFUME with Results from the AGR-1 Irradiation Experiment." INL/EXT-14-31975, Rev. 0, Idaho National Laboratory. <https://doi.org/10.2172/1164852>.
16. Skerjanc, W. F. 2020. "Comparison of Fission Product Release Predictions Using PARFUME With Results From the AGR-2 Irradiation Experiment." INL/EXT-20-59448, Rev. 0, Idaho National Laboratory.
17. "AGR-3/4 Irradiation Experiment Test Plan," PLN-3867, Rev. 1, Idaho National Laboratory, May 2015.
18. Pham, B. T., J. Palmer, D. W. Marshall, G. L. Hawkes, D. M. Scates, and P. A. Demkowicz. 2021. "AGR-5/6/7 Irradiation Test Final As-Run Report," INL/EXT-21-64221, Rev. 0, Idaho National Laboratory. <https://www.osti.gov/servlets/purl/1822435>.

19. Collin, B. P. 2012. "AGR-1 Safety Test Predictions using the PARFUME Code." INL/EXT-12-26014, Rev. 0, Idaho National Laboratory. <https://doi.org/10.2172/1048407>.
20. Collin, B. P. 2014. "AGR-2 Safety Test Predictions using the PARFUME Code." INL/EXT-14-33082, Rev. 0, Idaho National Laboratory. <https://doi.org/10.2172/1167547>.
21. Collin, B. P. 2014. "Comparison of Fission Product Release Predictions using PARFUME with Results from the AGR-1 Safety Tests." INL/EXT-14-31976, Rev. 0, Idaho National Laboratory. <https://doi.org/10.2172/1164853>.
22. Demkowicz, P. A., J. D. Hunn, R. N. Morris, I. Rooyen, T. Gerczak, J. M. Harp, S. A. Ploger. 2015. "AGR-1 Post-Irradiation Examination Final Report." INL/EXT-15-36407, Rev. 0, Idaho National Laboratory. <https://doi.org/10.2172/1236801>.
23. Stempien, J. D., J. D. Hunn, R. N. Morris, T. J. Gerczak, and P. A. Demkowicz. 2021. "AGR-2 TRISO Fuel Post-Irradiation Examination Final Report." INL/EXT-21-64279, Rev. 0, Idaho National Laboratory. <https://www.osti.gov/servlets/purl/1822447>.
24. Hunn, J. D., C. A. Baldwin, T. J. Gerczak, F. C. Montgomery, R. N. Morris, C. M. Silva, P. A. Demkowicz, J. M. Harp, S. A. Ploger, I. Rooyen, and K. E. Wright. 2016. "Detection and Analysis of Particles with Breached SiC in AGR-1 Fuel Compacts." *Nuclear Engineering and Design* 306: 36–46. <https://doi.org/10.1016/j.nucengdes.2015.12.011>.
25. Skerjanc, W. F. 2021. "AGR-5/6/7 Irradiation As-Run Predictions Using PARFUME." INL/EXT-21-64576, Rev. 0, Idaho National Laboratory. <https://www.osti.gov/servlets/purl/1826378>.
26. Dunzik-Gougar, M. L. 2019. "Measuring Mechanical Properties of Select Layers and Layer Interfaces of TRISO Particles via Micromachining and In-Microscope Tensile Testing." NEUP-19-17251, Idaho State University.
27. Zhang, Y. 2020. "Statistical Modeling of the Effect of Microstructural Heterogeneity on the Irradiation Behavior of TRISO Fuel Buffer Layer." NEUP-20-19556, University of Wisconsin-Madison.
28. Wirth, B. 2020. "Multi-physics Fuel Performance Modeling of TRISO-bearing Fuel in Advanced Reactor Environments." IRP-20-22094, University of Tennessee.
29. Hales, J. D., A. Toptan, W. Jiang, and B. W. Spencer. 2022. "Numerical Evaluation of AGR-2 Fission Product Release." *Journal of Nuclear Materials* 558: 153325. <https://doi.org/10.1016/j.jnucmat.2021.153325>.
30. Jiang, W., G. Singh, J. D. Hales, A. Toptan, B. W. Spencer, S. R. Novascone, S. L. N. Dhulipala, and Z. M. Prince. 2022. "Efficient High-fidelity TRISO Statistical Failure Analysis using Bison: Applications to AGR-2 Irradiation Testing." *Journal of Nuclear Materials* 562: 153585. <https://doi.org/10.1016/j.jnucmat.2022.153585>.
31. Skerjanc, W. F., J. T. Maki, B. P. Collin, and D. A. Petti. 2016. "Evaluation of Design Parameters for TRISO-coated Fuel Particles to Establish Manufacturing Critical Limits using PARFUME." *Journal of Nuclear Materials* 469: 99–105. <https://doi.org/10.1016/j.jnucmat.2015.11.027>.
32. Ploger, S. A., P. A. Demkowicz, J. D. Hunn, and J. S. Kehn. 2012. "Ceramographic Examinations of Irradiated AGR -1 Fuel Compacts." INL/EXT-12-25301, Rev. 1, Idaho National Laboratory. <https://doi.org/10.2172/1072396>.